

# Electrochemical behavior of SiO as an anode material for Na-ion battery

*Masahiro Shimizu<sup>a,b</sup>, Hiroyuki Usui<sup>a,b</sup>, Kohei Fujiwara<sup>a,b</sup>,  
Kazuya Yamane<sup>a,b</sup>, Hiroki Sakaguchi<sup>a,b,\*</sup>*

<sup>a</sup> *Department of Chemistry and Biotechnology, Graduate School of Engineering, Tottori University  
4-101 Minami, Koyama-cho, Tottori 680-8552, Japan*

<sup>b</sup> *Center for Research on Green Sustainable Chemistry, Tottori University  
4-101 Minami, Koyama-cho, Tottori 680-8552, Japan*

\*Corresponding author. Tel./Fax: +81-857-31-5265; E-mail: sakaguch@chem.tottori-u.ac.jp

## **Abstract**

Electrochemical behavior of SiO electrode as a Na-ion battery anode was investigated by using thick-film electrodes without any binder or conductive additive. The SiO electrode reacted with Na to exhibit a reversible capacity of over 200 mA h g<sup>-1</sup> at the first cycle, whereas Si electrode showed less capacity. We previously demonstrated that SiO being an amorphous material is composed of three-dimensional SiO<sub>4</sub> tetrahedral network similar to silica glass and Si clusters, and that the Si clusters are finely dispersed in the SiO<sub>4</sub> matrices. Given this characteristics, it is considered that the capacity obtained from the SiO originates from an alloying reaction of the Si clusters having a high surface energy with Na.

**Keywords:** Silicon monoxide; Na-ion battery; Thick-film; Gas-deposition

## 1. Introduction

A next-generation energy storage device that use Na-ion as the charge carrier, Na-ion battery (NIB), has attracted more and more attention because of its low cost and natural abundance of sodium [1]. Development of host materials which can absorb much Na per its formula weight has been needed to realize NIB with a higher energy density. From the perspective, most recent studies of negative electrodes have been focused on alloy-based materials. Germanium (Ge) [2], tin (Sn) [3,4], and antimony (Sb) [5] react with Na to form binary alloys, which provides high theoretical capacities of  $369 \text{ mA h g}^{-1}$  (NaGe),  $847 \text{ mA h g}^{-1}$  ( $\text{Na}_{3.75}\text{Sn}$ ), and  $660 \text{ mA h g}^{-1}$  ( $\text{Na}_3\text{Sb}$ ). It has been recognized that the group 14 elements with the exception of silicon (Si) are electrochemically active against Na. Despite the existence of NaSi and NaSi<sub>2</sub> phases [6,7], there has been no report on electrochemical reactions of Si with Na. If the formation of the NaSi alloy occurs, a specific capacity of  $954 \text{ mA h g}^{-1}$  could be achieved, and its specific capacity is more than three times as large as that of carbon-based materials [8]. In addition, the volumetric change ratio of 244% from Si to fully sodiated Si is relatively small compared with those of Sn (530%) [3] and Sb (390%) [5], which reduces a mechanical stress causing capacity fading. We guessed that the reason why the Na–Si alloying reaction does not electrochemically occur is due to the bulk-stated Si. Our group has previously demonstrated that SiO being an amorphous material is composed of three-dimensional SiO<sub>4</sub> tetrahedral network similar to silica (SiO<sub>2</sub>) glass and metallic Si clusters, and that the Si clusters are finely dispersed in the SiO<sub>4</sub> matrices [9]. We anticipated that the Si cluster with a high surface

energy is electroactive against Na to show a reversible capacity by the formation of the Na–Si alloy.

In this study, we investigated fundamental electrode properties of SiO as a Na-ion battery anode by using thick-film electrodes without any binder or conductive additive. To the best of our knowledge, this is the first report on an anode property of Si-based material.

## 2. Experimental

Granular silicon monoxide (SiO, Wako Pure Chemical Industries, Ltd., 99.9%) powder was pulverized by using a high-energy planetary ball mill (Classic Line P-6, FRITSCH) at 380 rpm to prepare an active material powder. The weight ratio of the balls to the powder was set to be 65:1, and the mechanical milling (MM) times were 10 min, 20 min, and 60 min. Crystal structures of these powders were investigated by an X-ray diffractometer (Ultima IV, Rigaku Co., Ltd.) with CuK $\alpha$  radiation and a Raman microscopy system (NanofinderFLEX, Tokyo Instruments, Inc.) with 532 nm line of Nd:YAG laser. The morphologies and particle sizes of the powders were observed by a field emission scanning electron microscope (FE-SEM, JSM-6701F, JEOL Ltd.).

SiO thick-film electrodes were prepared by a gas-deposition method through the use of helium carrier gas. Further detailed conditions are described in our previous reports [4,10]. The deposition area is *ca.* 0.5 cm<sup>2</sup>, and the weight of the deposited active material on the substrate was measured to an accuracy of 1  $\mu$ g by ultra-microbalance (XP6, METTLER TOLEDO) equipped with an anti-vibration table. A typical film thickness was confirmed to be *ca.* 8.0  $\mu$ m by observation using a

confocal scanning laser microscope (CSLM, VK-9700, Keyence) [11]. 2032-type coin cells were fabricated from SiO thick-film electrode as working electrode, Na foil as counter electrode, electrolyte of 1.0 M sodium bis(trifluoromethanesulfonyl)amide (NaTFSA)-dissolved in propylene carbonate (PC) (Kishida Chemical Co., Ltd.), and propylene-based separator. To evaluate electrochemical Na-insertion/extraction properties of SiO electrode, galvanostatic charge–discharge cycling tests were performed using an electrochemical measurement system (HJ-1001 SD8, Hokuto Denko Co., Ltd.) in the potential range between 0.005 and 3.000 V vs. Na/Na<sup>+</sup> at 303 K. The current density was set to 50 mA g<sup>-1</sup>.

### 3. Results and discussion

SiO powders underwent pulverization of an agglomeration (Figs. S1 and S2) by a high-energy ball milling to prepare active material powders. In the milled SiO samples for 10 min and 20 min, their particles have similar morphologies with the range from submicrometer to 5 μm as observed in Fig. 1a. On the other hand, the size in SiO powder for 60 min-milling is much smaller with several hundred nanometer. Although a broad peak indicating SiO was only detected in a pristine sample (not shown here), a diffraction peak originated from Si began appearing at 47.3° in 10 min-milling SiO sample (Fig. 1b), and its peak intensity significantly increased with milling time. In the 60 min-milling sample, the existence of Si is apparent, which means a disproportional reaction of SiO to Si and amorphous SiO<sub>x</sub>/SiO<sub>2</sub> [12,13].

Fig. 2a compares Raman spectra of pure Si and SiO electrodes. In the Raman spectrum of as-prepared Si electrode, a relatively sharp peak was observed at  $520\text{ cm}^{-1}$ . This result indicates that the electrode is composed only of crystalline Si. Meanwhile the electrode consisted of 10 min-milling SiO powder showed a peak at  $498\text{ cm}^{-1}$ . This is attributed to transverse optical (TO) mode from microcrystalline ( $\mu c$ )-Si which typically consists of small grains with 20–30 nm in size [14,15]. As is clear from Fig. 1c, the peak position of TO mode corresponding to  $\mu c$ -Si shifted from  $498\text{ cm}^{-1}$  to  $505\text{ cm}^{-1}$  with increasing the milling time, which suggests that crystal growth of  $\mu c$ -Si grains, disproportional reaction of SiO, occurred during ball-milling. This agrees with the result obtained from the XRD measurements. Fig. 2b represents initial charge–discharge (Na insertion–extraction) curves of the Si electrode and the SiO electrodes. The Si electrode brought no potential plateau and showed only a little reversible capacity. Furthermore, no capacity increasing was found even when using an electrode consisted of a nano-sized Si powder (Fig. S3). The charge and discharge capacities are due to an electrolyte decomposition. From these result, it is implied that sodiation of crystalline Si ( $c$ -Si) is an electrochemically-unfavorable reaction at room temperature if not inactive. Komaba *et al.* have reported that an alloying reaction of  $c$ -Si with Na hardly occurs [16], and Obrovac *et al.* have demonstrated that XRD patterns of Si electrodes did not change during electrochemical tests at 333 K [17]. In contrast to these Si electrodes, potential plateaus at around 0.1 V vs. Na/Na<sup>+</sup> can be confirmed on the Na-insertion curves in all of the SiO electrodes in this study. Their initial discharge (Na-extraction) capacities in the 10 min, 20 min, and 60 min-milling

electrodes were 220 mA h g<sup>-1</sup>, 170 mA h g<sup>-1</sup>, and 80 mA h g<sup>-1</sup>, respectively. Note that the reversible capacity decreased as the peak position in Raman spectra of SiO electrodes shifts to higher wavenumber side. In other words, a larger capacity were achieved when a degree of the disproportionation reaction is smaller. From this tendency, it is expected that a highest capacity can be achieved from SiO which does not disproportionate. However, since pristine SiO granule is an improper size (diameter: 2–3 mm) for utilizing as an active material, we pounded it in a mortar and prepared an electrodes composed of its crushed SiO granule. The electrode showed a reversible capacity of 180 mA h g<sup>-1</sup> at the first cycle (Fig. S4), which was greater than any other electrode excluding the 10 min-milling electrode. The relatively small capacity is attributed mainly to its large particle size of crushed SiO granule (diameter: 30–200 μm). Considering the experimental results and the characteristic of the SiO structure [9,18], possible reactions of SiO with Na are one or more of following: (i) conversion reactions of sodium silicates such as Na<sub>2</sub>SiO<sub>3</sub>, Na<sub>4</sub>SiO<sub>4</sub>, Na<sub>2</sub>Si<sub>2</sub>O<sub>5</sub>, and Na<sub>2</sub>Si<sub>4</sub>O<sub>9</sub>, (ii) alloying and dealloying reactions between Na and Si finely dispersed in the SiO<sub>4</sub> matrix. In the case of SiO as a Li-ion battery anode, SiO<sub>2</sub> in its structure reacts with Li to irreversibly form Li<sub>2</sub>O or/and Li<sub>4</sub>SiO<sub>4</sub> compounds [19]. From the viewpoint of the monovalent alkali metal, the sodiation of SiO<sub>2</sub> is presumably an irreversible reaction as with the Li-ion battery system. On the other hand, Han *et al.* have performed an atom-level assessment of amorphous Si (*a*-Si) as a Na-ion battery anode using ab initio molecular dynamics simulations [20]. According to their calculations, *a*-Si can absorb 0.76 Na atoms per Si, and the Na<sub>0.76</sub>Si formed below 0.1 V vs. Na/Na<sup>+</sup> delivers a

specific capacity of  $725 \text{ mA h g}^{-1}$ . We therefore prepared an *a*-Si electrode by an electrochemical method, and experimentally investigated its charge–discharge behavior at a relatively high temperature (Fig. S5). Contrary to our expectation, the capacity of only  $90 \text{ mA h g}^{-1}$  was obtained, and it was far from the theoretical capacity calculated by Han *et al.* though the capacity is slightly larger than that of the *c*-Si electrode. This much lower utilization of the active material is probably due to the bulk property. As was mentioned before, Si in SiO structure exists as a cluster under the state of finely dispersing in SiO<sub>4</sub> matrix (Fig. S6). From this, it is quite likely that the Si is activated and its reactivity to Na is enhanced.

In order to investigate a correlation between crystallite sizes of Si and reversible capacities obtained from the SiO electrodes, the sizes of Si in SiO were calculated from respective peak width of (331) plane in XRD patterns measured at a scan rate of  $0.2^\circ \text{ min}^{-1}$  (Fig. S7). Fig. 3a shows the correlation between initial capacities and MM times to SiO powder. The reversible capacity tends to decrease with the MM processing times. An important point to be emphasized is that the capacities of the SiO electrodes become larger when the crystallite size of Si is smaller, as shown in Fig. 3b, which indicates that dispersed Si in SiO<sub>4</sub> matrix reacts with Na to electrochemically form Na–Si binary alloy. At the same time, from the increase in the crystallite size of Si by the mechanical milling, we consider that Si which existed as a cluster gradually agglutinated to become a bulk state and thereby reduced the activity against Na. Incidentally, the crystallite size of pure Si was 44 nm. Since SiO material consists of an equimolar mixture of elemental Si and SiO<sub>2</sub>, the weight ratio of Si to

SiO<sub>2</sub> corresponds to 32/68 wt.%. If only the Si is assumed to be active against Na to form the Na<sub>0.76</sub>Si alloy, the calculated theoretical capacity of SiO is 232 mA h g<sup>-1</sup> {= 725 mA h g<sup>-1</sup> (Na<sub>0.76</sub>Si) × 0.32 (weight ratio of Si in SiO)}. This value is agreement with the reversible capacity (220 mA h g<sup>-1</sup>) obtained in 10 min-milling SiO electrode, which also suggests a possibility of Na–Si alloying and dealloying reactions. Although it is still unclear whether an irreversible capacity of SiO electrode during the first cycle classified into an electrolyte decomposition or an irreversible sodiation of SiO<sub>2</sub> such as the formation of sodium silicate, we guess that Si cluster in SiO reacted with Na to electrochemically form the binary alloy. We are now working on elucidation of the reaction mechanism of SiO as a Na-ion battery anode by using XRD and Raman spectroscopy, and will report it in a future article.

Figs. 4a and 4b show dependence of discharge capacities and coulombic efficiencies on cycle number for the SiO electrodes and the Si electrode. The 10 min, 20 min, and 60 min-milling SiO electrodes exhibited discharge capacities of 170 mA h g<sup>-1</sup>, 130 mA h g<sup>-1</sup>, and 40 mA h g<sup>-1</sup>, respectively, at the 100th cycle. In every case, the capacity retention was *ca.* 77%. These SiO electrodes showed low efficiencies within the range of 55–43% at the first cycle, but the efficiencies were improved to 100% after the ninth cycle with the exception of the 60-min milling SiO electrode. Meanwhile, the Si electrode had only ~20 mA h g<sup>-1</sup> through charge–discharge cycling test. The electrodes composed of Si with a large crystallite size, 60 min-milling SiO electrode and Si electrode, showed low efficiencies below 93% and 80% until the initial tenth cycle. This behavior is assigned

to continuous decomposition of electrolyte. In order to improve the cycling performance of the SiO electrode, we searched for an optimized electrolyte from among commercially-available electrolyte products. As a result, the electrolyte consisting of NaTFSA and PC yielded the best anode property compared with those in 1.0 M NaPF<sub>6</sub>/EC:DEC (50:50 vol.%), 1.0 M NaFSA/PC, and 4.8 M NaTFSA/DME (Fig. S8).

#### **4. Conclusions**

We investigated the electrochemical behavior of SiO as a Na-ion battery anode without any binder or conductive additive. It was found that SiO reacts with Na to reversibly show Na-insertion/extraction capacities. The electrode composed of SiO powder milled for 10 min exhibited the Na-extraction capacity of 220 mA h g<sup>-1</sup> at the first cycle, whereas the Si electrode showed less capacity. The possible reaction mechanism of SiO with Na is following: finely dispersed Si in the SiO<sub>4</sub> matrix, the Si having high activity in comparison to bulk Si, absorbs Na to form Na–Si binary alloy. The 10 min-milling SiO electrode delivered the capacity of 170 mA h g<sup>-1</sup> at the 100th cycle with the high capacity retention of 77%, which indicates that SiO is a promising candidate as an active material for NIB. To realize a further increase in capacity of Si-based electrode, the use of an *a*-Si with a small grain would be effective.

#### **Acknowledgments**

M. Shimizu thanks Japan Society for the Promotion of Science (JSPS) for research fellowship (No. 2611485). The authors gratefully acknowledge Prof. Y. Domi and Mr. S. Morishita for their helpful comments. The authors thank Dr. H. Furutani (KANEKA Co., Japan) for supplying chemicals.

## References

- [1] N. Yabuuchi, K. Kubota, M. Dahbi, S. Komaba, *Chem. Rev.* 114 (2014) 11636.
- [2] P.R. Abel, Y.-M. Lin, T. de Souza, C.-Y. Chou, A. Gupta, J.B. Goodenough, G.S. Hwang, A. Heller, C.B. Mullins, *J. Phys. Chem. C* 117 (2013) 18885.
- [3] T. Yamamoto, T. Nohira, R. Hagiwara, A. Fukunaga, S. Sakai, K. Nitta, S. Inazawa, *J. Power Sources* 217 (2012) 479.
- [4] M. Shimizu, H. Usui, H. Sakaguchi, *J. Power Sources* 248 (2014) 378.
- [5] L. Xiao, Y. Cao, J. Xiao, W. Wang, L. Kovarik, Z. Nie, J. Liu, *Chem. Commun.* 48 (2012) 3321.
- [6] J. Sangster, A. D. Pelton, *J. Phase Equilib.* 13 (1992) 67.
- [7] H. Morito, T. Yamada, T. Ikeda, H. Yamane, *J. Alloys Comp.* 480 (2009) 723.
- [8] S. Komaba, W. Murata, T. Ishikawa, N. Yabuuchi, T. Ozeki, T. Nakayama, A. Ogata, K. Gotoh, K. Fujiwara, *Adv. Energy Mater.* 21 (2011) 3859.
- [9] Y. Nagao, H. Sakaguchi, H. Honda, T. Fukunaga, T. Esaka, *J. Electrochem. Soc.* 151 (2004) A1572.

- [10]M. Shimizu, H. Usui, K. Matsumoto, T. Nokami, T. Itoh, H. Sakaguchi, *J. Electrochem. Soc.* 161 (2014) A1765.
- [11]M. Shimizu, H. Usui, T. Suzumura, H. Sakaguchi, *J. Phys. Chem. C* 119 (2015) 2975.
- [12]J.I. Lee, K.T. Lee, J. Cho, J. Kim, N.S. Choi, S. Park, *Angew. Chem. Int. Ed.* 51 (2012) 2767.
- [13]J.-H. Kim, H.-J. Sohn, H. Kim, G. Jeong, W. Choi, *J. Power Sources* 170 (2007) 456.
- [14]T. Kim, S. Park, S.M. Oh, *J. Electrochem. Soc.* 154 (2007) A1112.
- [15]V. M. Marchenko, V. V. Koltashev, S. V. Lavrishchev, D. I. Murin, V. G. Plotnichenko, *Laser Physics* 10 (2000) 576.
- [16]S. Komaba, Y. Matsuura, T. Ishikawa, N. Yabuuchi, W. Murata, S. Kuze, *Electrochem. Commun.* 12 (2012) 65.
- [17]L.D. Ellis, B.N. Wilkes, T.D. Hatchard, M.N. Obrovac, *J. Electrochem. Soc.* 161 (2014) A416.
- [18]H. Yamamura, K. Nobuhara, S. Nakanishi, H. Iba, S. Okada, *J. Ceram. Soc. Japan* 119 (2011) 855.
- [19]N. Yan, F. Wang, H. Zhong, Y. Li, Y. Wang, L. Hu, Q. Chen, *Sci. Rep.* 3 (2013) 1568.
- [20]S.C. Jung, D.S. Jung, J.W. Choi, Y.-K. Han, *J. Phys. Chem. Lett.* 5 (2014) 1283.

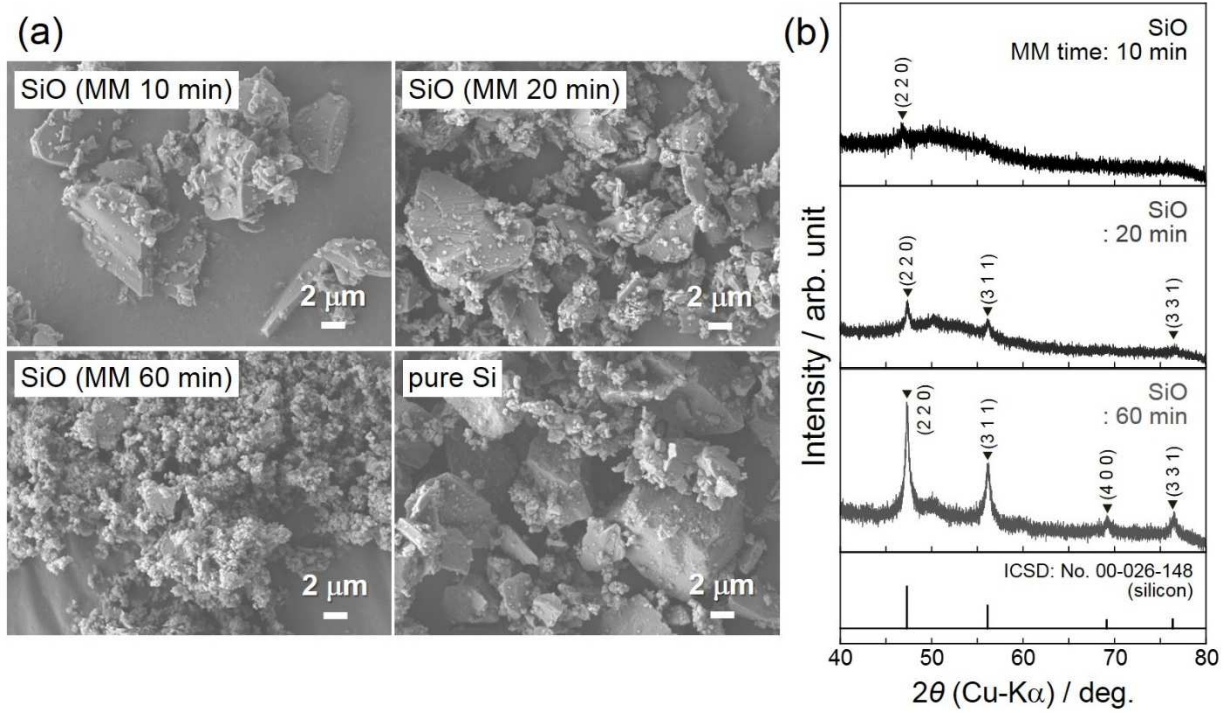


Fig. 1 (a) FE-SEM images of milled SiO and pure Si powders. (b) XRD patterns of SiO powders prepared by mechanical milling for 10 min, 20 min, and 60 min.

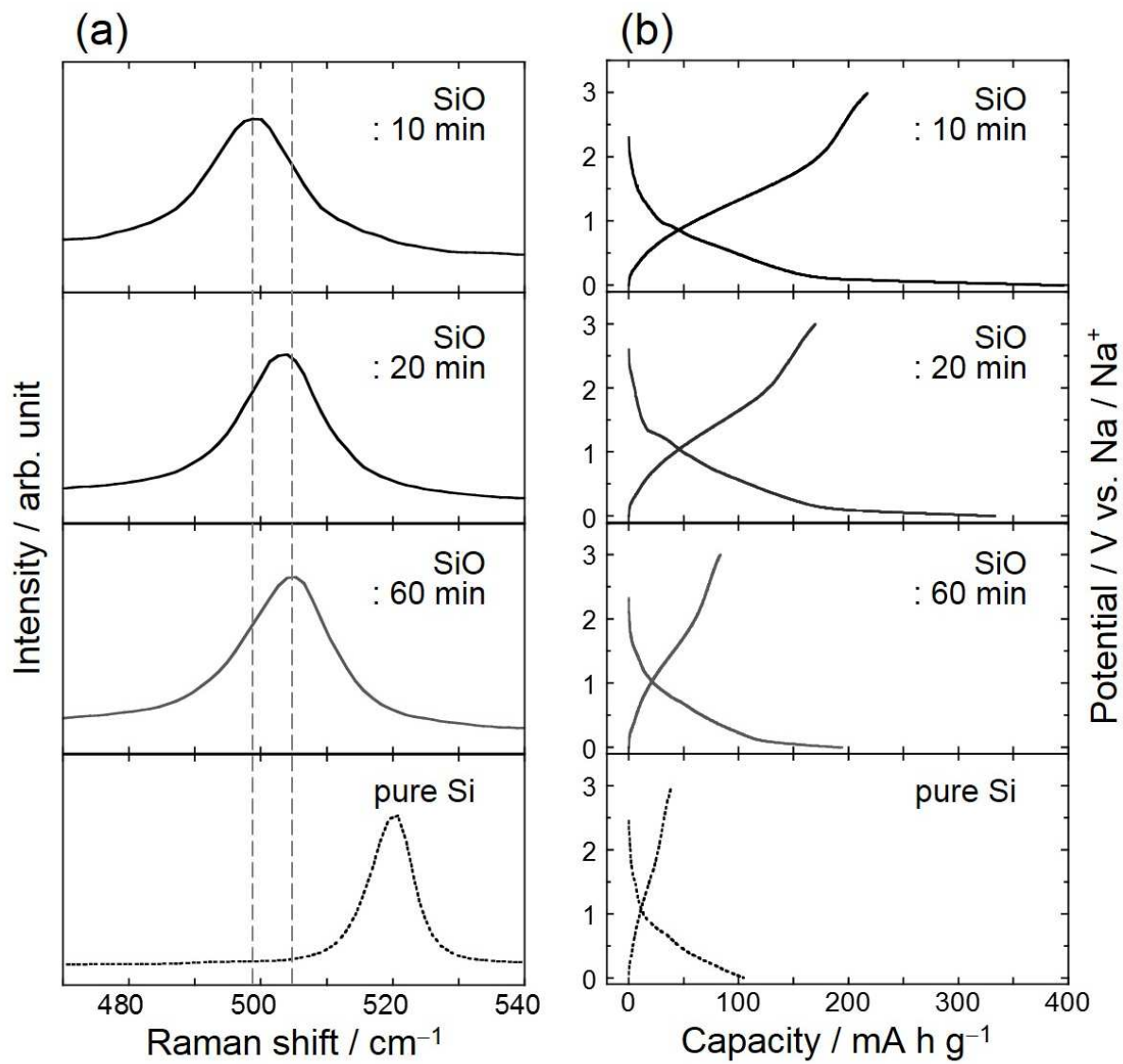


Fig. 2 (a) Raman spectra and (b) initial charge–discharge (Na insertion–extraction) behaviors of SiO and Si electrodes.

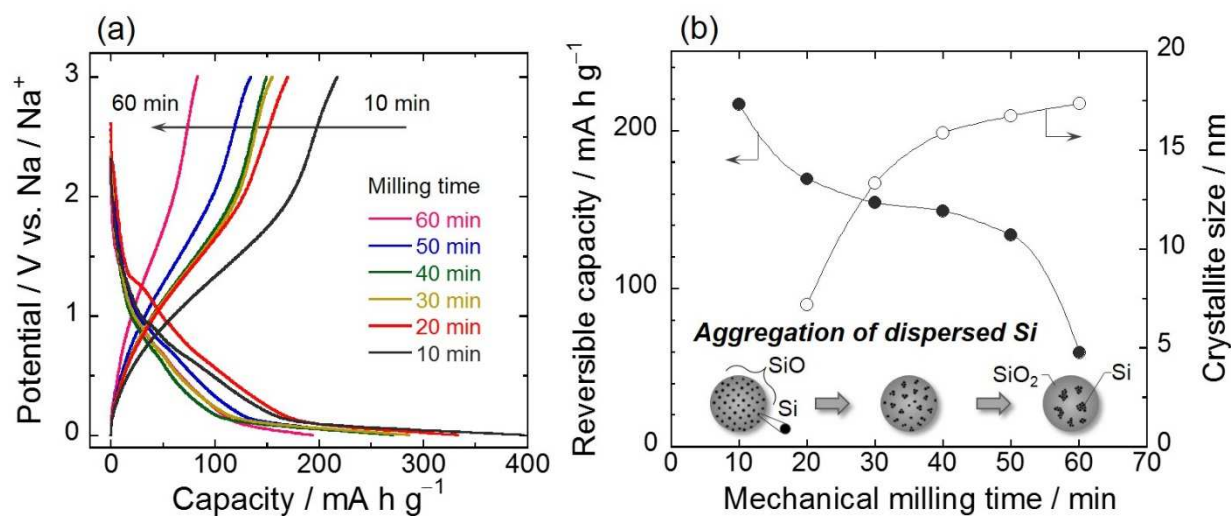


Fig. 3 (a) Na-insertion/extraction profiles of thick-film electrodes consisted of milled SiO powders for various times. (b) Correlation between crystallite sizes of Si and reversible capacities obtained from the SiO electrodes at the first cycle. The crystallite sizes of Si were calculated from the Scherrer's equation using a peak width located at  $76.4^\circ$  (Si, (3 3 1) plane) in respective XRD patterns measured at a scan rate of  $0.2^\circ \text{ min}^{-1}$ . The crystallite size of pure Si used in this study was 44 nm.

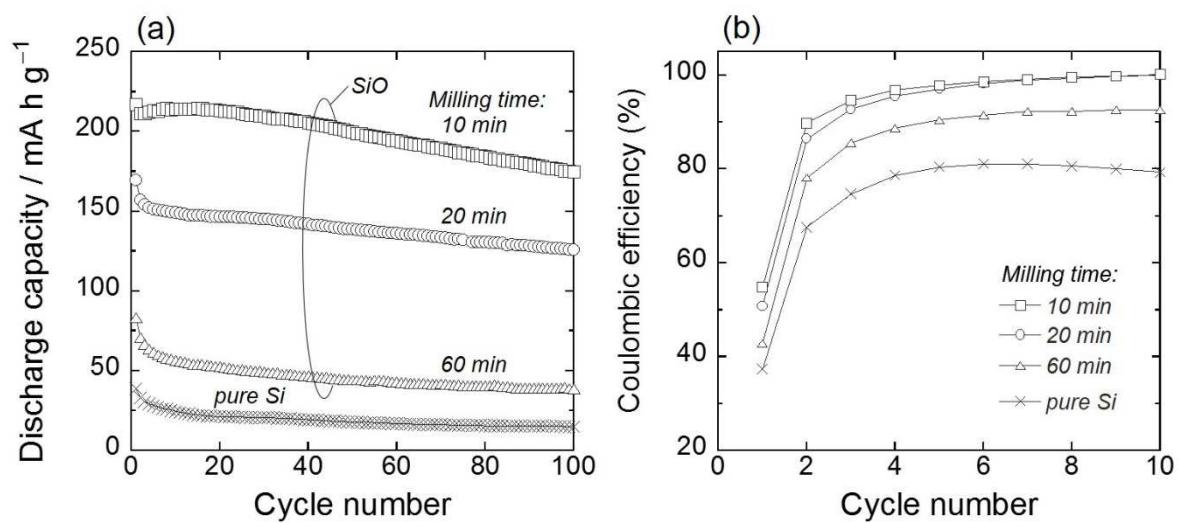


Fig. 4 (a) Cycle performance of electrodes consisted of milled SiO powder at various times. For comparison, the performance of Si electrode was plotted. (b) Variation in coulombic efficiencies in the initial 10th cycle for their electrodes.

## Figure caption

Fig. 1 (a) FE-SEM images of milled SiO and pure Si powders. (b) XRD patterns of SiO powders prepared by mechanical milling for 10 min, 20 min, and 60 min.

Fig. 2 (a) Raman spectra and (b) initial charge–discharge (Na insertion–extraction) behaviors of SiO and Si electrodes.

Fig. 3 (a) Na-insertion/extraction profiles of thick-film electrodes consisted of milled SiO powders for various times. (b) Correlation between crystallite sizes of Si and reversible capacities obtained from the SiO electrodes at the first cycle. The crystallite sizes of Si were calculated from the Scherrer's equation using a peak width located at  $76.4^\circ$  (Si, (3 3 1) plane) in respective XRD patterns measured at a scan rate of  $0.2^\circ \text{ min}^{-1}$ . The crystallite size of pure Si used in this study was 44 nm.

Fig. 4 (a) Cycle performance of electrodes consisted of milled SiO powder at various times. For comparison, the performance of Si electrode was plotted. (b) Variation in coulombic efficiencies in the initial 10th cycle for their electrodes.